NJC

Accepted Manuscript

This is an *Accepted Manuscript*, which has been through the Royal Society of Chemistry peer review process and has been accepted for publication.

Accepted Manuscripts are published online shortly after acceptance, before technical editing, formatting and proof reading. Using this free service, authors can make their results available to the community, in citable form, before we publish the edited article. We will replace this *Accepted Manuscript* with the edited and formatted *Advance Article* as soon as it is available.

You can find more information about *Accepted Manuscripts* in the Information for Authors.

Please note that technical editing may introduce minor changes to the text and/or graphics, which may alter content. The journal's standard Terms & Conditions and the Ethical guidelines still apply. In no event shall the Royal Society of Chemistry be held responsible for any errors or omissions in this *Accepted Manuscript* or any consequences arising from the use of any information it contains.

ROYAL SOCIETY OF CHEMISTRY

www.rsc.org/njc

Cite this: DOI: 10.1039/c0xx00000x

www.rsc.org/njc

PAPER

Facile synthesis of mesoporous cobalt oxide rugby balls for electrochemical energy storage

Yuting Hao, Huanwen Wang, Zhonghua Hu, Lihua Gan, Zijie Xu*

Received (in XXX, XXX) Xth XXXXXXXXX 20XX, Accepted Xth XXXXXXXXX 20XX

DOI: 10.1039/b000000x

Mesoporous Co_3O_4 rugby balls were firstly obtained by utilizing a facile two-step method. This unique morphology together with the mesoporous feature manifests excellent capacitive performance (an energy density (14.3 Wh kg^{-1}), a power density (7503 W kg^{-1}) and no decay after 10,000 cycles) for constructing the Co_3O_4 rugby balls//graphene hydrogels asymmetric supercapacitor.

As a class of energy storage device with properties intermediate to those of batteries and electrostatic capacitors, supercapacitors display the desirable properties of high power density (ten times more than batteries), fast rates of charge-discharge (with seconds), excellent cycling stability, small size, low mass and low maintenance cost [1–3]. However, the energy storage density of existing supercapacitors is limited, generally an order of magnitude lower than that of batteries. Currently, improving the energy density while maintaining the high power density and cycling stability for supercapacitor devices remains a primary research focus in the field [4, 5].

Pseudocapacitive transition-metal oxides such as RuO_2 [6], NiO [7], Co_3O_4 [8], Bi_2O_3 [9] and MnO_2 [10], have been studied extensively as active electrode materials for supercapacitors owing to their high energy density and large charge transfer-reaction pseudocapacitance which is based on fast and reversible redox reactions at the electrode surface, resulting in much higher specific capacitance exceeding that of carbon-based materials. Among them, Co_3O_4 is considered to be the most attractive oxide material due to its abundance, low cost, higher surface area, good redox property, controllable size and shape, and structural identities [11-13]. Recent works have shown supercapacitor applications of different Co_3O_4 nanostructures, including hollow sphere (346 F g^{-1}) [14], porous film (454 F g^{-1} at 2 A g^{-1}) [15], nanotubes (574 F g^{-1} at 0.1 A g^{-1}) [16], nanowires (1160 F g^{-1} at 2 A g^{-1}) [17], rectangular 2D flakes (548 F g^{-1} at 8 A g^{-1}) [18], hollow boxes (278 F g^{-1} at 0.5 A g^{-1}) [19], aerogels (623 F g^{-1}) [20], nanocone arrays (562 F g^{-1} at 2 A g^{-1}) [21], interconnected nanoflake film [22]. As the capacitive phenomenon is directly associated with surface properties, any change in the surface morphology of the sample greatly influences its electrochemical performance. Toward theoretical Faradic capacitance, seeking for a highly novel microstructure for Co_3O_4 has still been expected.

In this work, mesoporous Co_3O_4 rugby balls have been successfully and firstly prepared via a facile two-step method using Polyvinylpyrrolidone (PVP) as the structure-directing reagent. When used as supercapacitor electrodes, such particular morphology together with the mesoporous microstructure gives excellent capacitive performance during the charge-discharge and thus promising application as supercapacitors. On the basis of the as-prepared Co_3O_4 rugby balls and 3D conductive graphene hydrogels, an asymmetric supercapacitor is constructed and high energy density and power density as well as long cycling performance have been demonstrated.

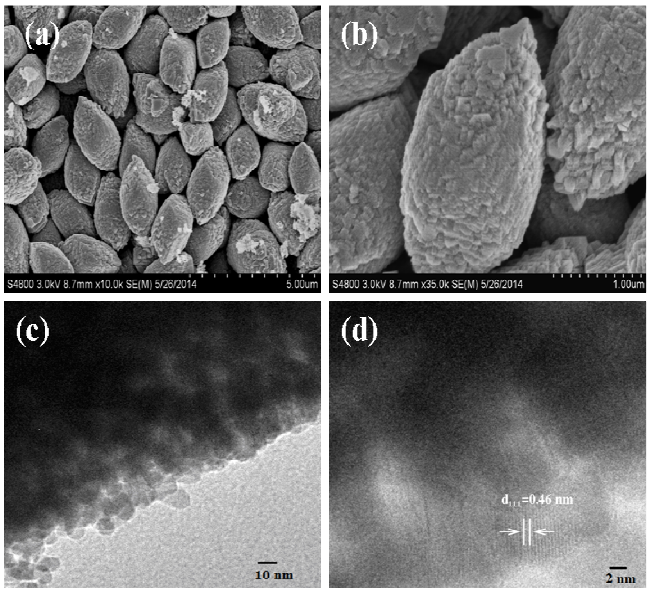

Fig. 1. (a-b) FESEM and (c-d) TEM images of mesoporous cobalt oxide rugby balls.

The surface morphology of as-synthesized Co_3O_4 is characterized by FESEM. Fig. 1a-1b shows low- and high-magnification FESEM images. It is observed that the Co_3O_4 sample presents the uniform rugby ball morphology. The size of single Co_3O_4 rugby ball is 1 μm and 2 μm in the transverse and longitudinal direction, respectively. Form TEM images, it can be see that each rugby ball consists of numerous interconnected nanoparticles forming a mesoporous structure, which is generated during the thermal treatment (Fig. 1c). The high-resolution TEM (HRTEM) image shown in Fig. 1d further reveals these Co_3O_4 nanoparticles with a size of ca. 10 nm and

the existence of interparticle mesopores with a size ranging from 2 to 5 nm. The lattice fringes show an interplanar spacing of ca. 0.46 nm (Fig. 1d), corresponding to the (111) plane of the cubic Co_3O_4.

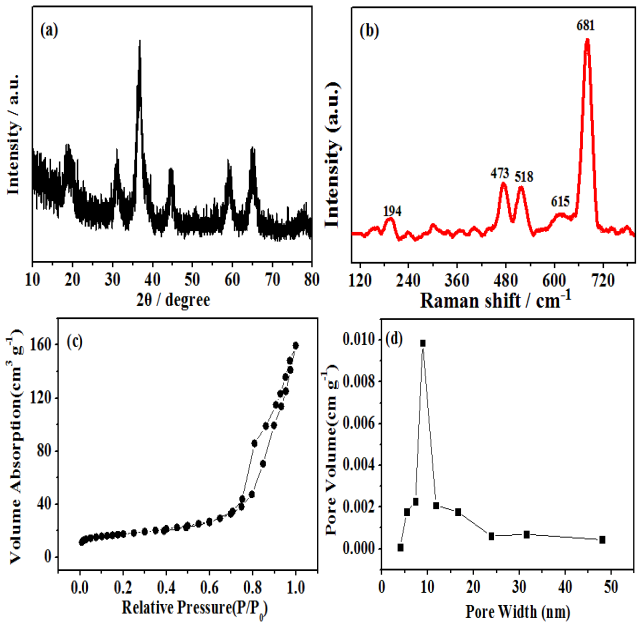

Fig. 2. (a) XRD patterns, (b) Raman spectrum, (c) Nitrogen adsorption and desorption isotherms and (d) BJH pore size distribution for mesoporous cobalt oxide rugby balls.

From the XRD pattern (Fig. 2a), it can be seen that the sample shows typical diffraction peaks of Co_3O_4 phase (JCPDS, No. 43-1003). From Fig 2b, five distinguishable Raman bands are located at approximately 194, 473, 518, 615, and 681 cm-1, which correspond to the F2g, Eg, F2g, F2g and A1g modes, respectively, of the crystalline Co_3O_4 phase in agreement with the literature values [23]. From the N_2 adsorption-desorption isotherm of the Co_3O_4 rugby balls (Fig. 2c), it can be seen that a distinct hysteresis loop can be found with typical IV sorption behavior, indicating the existence of a typical mesoporous microstructure. The pore-size-distribution data (Fig. 2d) shows that the size of majority of the pores is focused on the 8.9 nm. The mesoporosity is assigned to the thermal decomposition of the starting material, which could result in weight loss and volume shrinking. The mesoporous structure gives rise to a relatively high Brunauer-Emmett-Teller (BET) specific surface area of 61 $m^2\ g^{-1}$.

Such unique Co_3O_4 rugby ball morphology coupled with the mesoporous structure and high surface area are beneficial to ion transport in the electrode/electrolyte. The electrochemical performance is obtained by cyclic voltammetry (CV) and galvanostatic charge–discharge measurements. From CV curves (Fig. 3a), there are two redox peaks due to the following faradaic reactions [24-26]:

$$Co_3O_4 + OH^- \leftrightarrow 3CoOOH + e^- \quad (1)$$

$$CoOOH + OH^- \leftrightarrow CoO_2 + H2O + e^- \quad (2)$$

Fig. 3b presents galvanostatic charge-discharge curves of the mesoporous Co_3O_4 rugby balls at different current densities. The specific capacitance is shown as a function of the current density in Fig. 3c. At 1 A g^{-1}, Co_3O_4 rugby balls have a capacitance value of 480 F g^{-1}. Even at the high specific current of 10 Ag^{-1}, there is still 64% capacitance retention, which is indicative of excellent rate property for the Co_3O_4 rugby ball electrode. The excellent cycle stability is demonstrated in Fig. 3d. At a cycle number of 150, the capacitance value increases 18% because of sample activation. After a 3000-cycle test, the capacity retains 84% of the initial value.

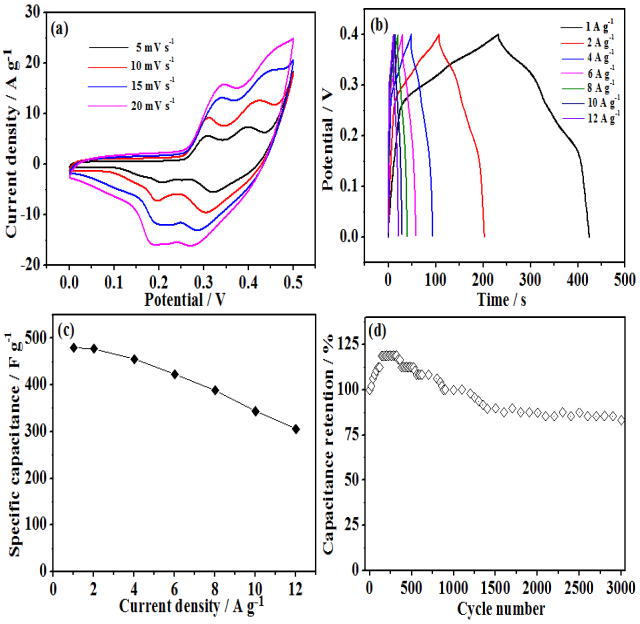

Fig. 3. (a) CV curves, (b) charge–discharge curves, (c) capacitances versus current densities and (d) variation of capacitance with cycle number at 4 A g–1 of mesoporous cobalt oxide rugby balls.

To further investigate the practical application of the sample in electrochemical energy storage, we construct a novel asymmetric supercapacitor in aqueous KOH solution. The positive electrode is the Co_3O_4 rugby balls. In addition, considering the multiple advantages of graphene hydrogels in comparison with other carbon materials, including high surface-area-to-volume ratios, enhanced transport property and mechanical flexibility, it is worthwhile to select graphene hydrogels as the negative electrode for the asymmetric capacitor. From the FESEM images, it can be seen that graphene hydrogels have a macroporous morphology with the framework network (Fig. 4a). In the potential range from -0.9 to 0 V at a scan rate of 5 to 50 mV s^{-1}, CV curves of graphene hydrogels exhibit typical rectangular shape, which shows good charge propagation at the electrode surface (Fig. 4b). According to the charge-discharge curves (Fig. 4c), the specific capacitance of graphene hydrogels is calculated to be 200 F g^{-1} at a current density of 1 A g^{-1}. More importantly, graphene hydrogels still have a capacitance of 138 F g^{-1} at 20 A g^{-1} with the 56 % retention relative to 1 A g^{-1}. These capacitance performances are superior to previous activated carbon (AC) [27].

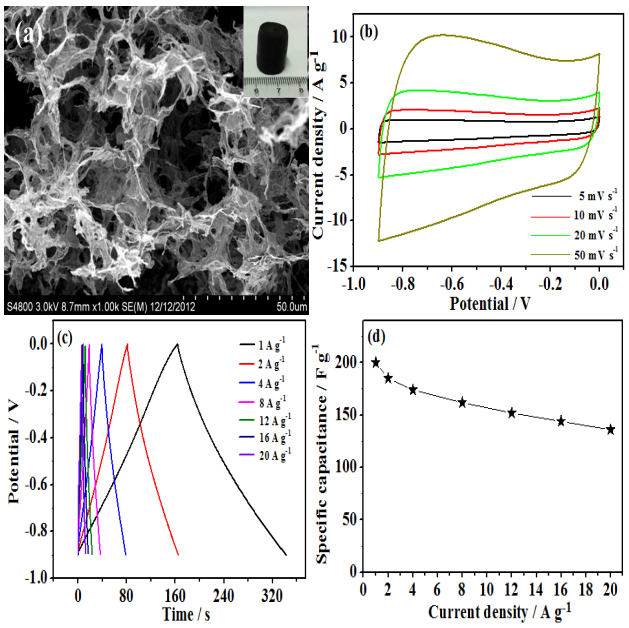

Fig. 4. (a) FESEM images, (inset) the photograph, (b) CV curves, (c) charge–discharge curves, and (d) capacitances versus current densities of graphene hydrogels.

On the basis of the Co_3O_4 rugby balls (positive) and graphene hydrogels (negative), the asymmetric supercapacitor is constructed in 1 M KOH solution (Fig. 5). The asymmetric supercapacitors usually consist of a Faradaic electrode (as the energy source) and a capacitor-type electrode (as the power source), which can make full use of the different potential windows of the two electrodes to provide a maximum operation voltage in the cell system, and accordingly result in a greatly improved energy density. For asymmetric supercapacitors, it is well-known that the charge balance between the two electrodes will follow the relationship $q_+ = q_-$, where the charge stored by each electrode usually depends on the specific capacitance (C), the potential range for the charge/discharge process (ΔE), and the mass of the electrode (m) following Equation: $q = C \times \Delta E \times m$ and in order to obtain $q_+ = q_-$, the mass balancing will be expressed as follows:

$$\frac{m_+}{m_-} = \frac{C_- \times \Delta E_-}{C_+ \times \Delta E_+} \qquad (3)$$

Based on the above analysis of the specific capacitance values and potential ranges found for the Co_3O_4 rugby balls and porous graphene hydrogels, the optimal mass ratio between the two electrodes should be $m_{(Co3O4)}/m_{(graphene)}$ = 1 in the asymmetric supercapacitor cell.

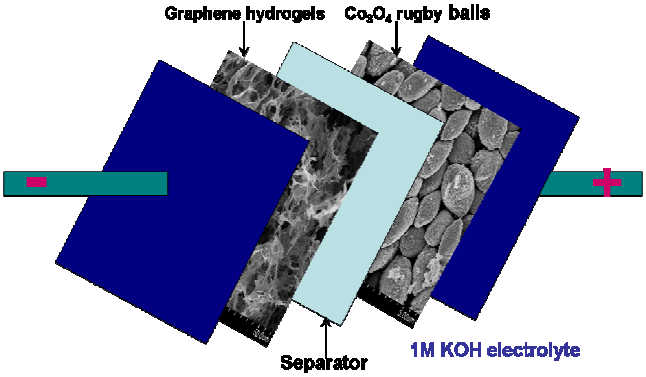

Fig. 5. Schematic of the assembled structure of the Co_3O_4 rugby balls//graphene hydrogels asymmetric supercapacitor.

The electrochemical performance of the Co_3O_4 rugby balls//graphene hydrogels asymmetric supercapacitor is shown in Fig. 6. The operating cell voltage can be extended to approximately 1.5 V. Obvious redox peaks are observed (Fig. 6a), indicating the Faradaic pseudocapacitive nature of the Co_3O_4 rugby balls//graphene hydrogels capacitor arising from the Co_3O_4 rugby ball electrode. All the discharge curves are nearly symmetric to their corresponding charging counterparts (Fig. 6b, 6c), suggesting an excellent electrochemical reversibility. The relationship between specific capacitance and current density is illustrated in Fig. 6d. The energy density, $E=[C(\Delta V)^2]/2$, and power density, $P=E/\Delta t$, are two important parameters that characterize supercapacitor, where C, ΔV and Δt are specific capacitance, potential window and discharge time, respectively [28, 29]. The calculation is base on the total mass of the positive (the Co_3O_4 rugby balls) and negative (graphene hydrogels) electrodes. Fig. 6e presents a Ragone plot, which relates the energy density to the power density of the asymmetric capacitor. The energy density decreases from 14.3 to 5 Wh kg^{-1} as the power density increases from 185 to 7503 W kg^{-1}. Noticeably, the energy density of 14.3 Wh kg^{-1} is much higher than that of symmetrical supercapacitors based on hydrazine reduced graphene hydrogels (5.7 Wh kg^{-1}) [30]. Furthermore, after a 10,000-cycle test at 4 A g^{-1}, the Co_3O_4 rugby balls//graphene hydrogels supercapacitor shows no obvious decay (Fig. 5f). This cycling performance is superior to most of previous reported samples including $Ni(OH)_2$//AC (82% retention after 1000 cycles)[31], graphene/MnO_2//graphene (79% retention after 1000 cycles)[32], $NiCo_2O_4$–rGO//AC (83% after 2500 cycles)[33]. EIS measurements after 1st and 10000th cycle are performed at 1.2 V. As shown in the inset of Fig. 6f, the impedance plots of the asymmetric supercapacitor show no obvious difference after 10000th cycle. This further indicates that repetitive cycling does not induce noticeable degradation of the microstructure. These superior electrochemical performances may be due to the synergistic effect of the Co_3O_4 rugby balls and graphene hydrogels.

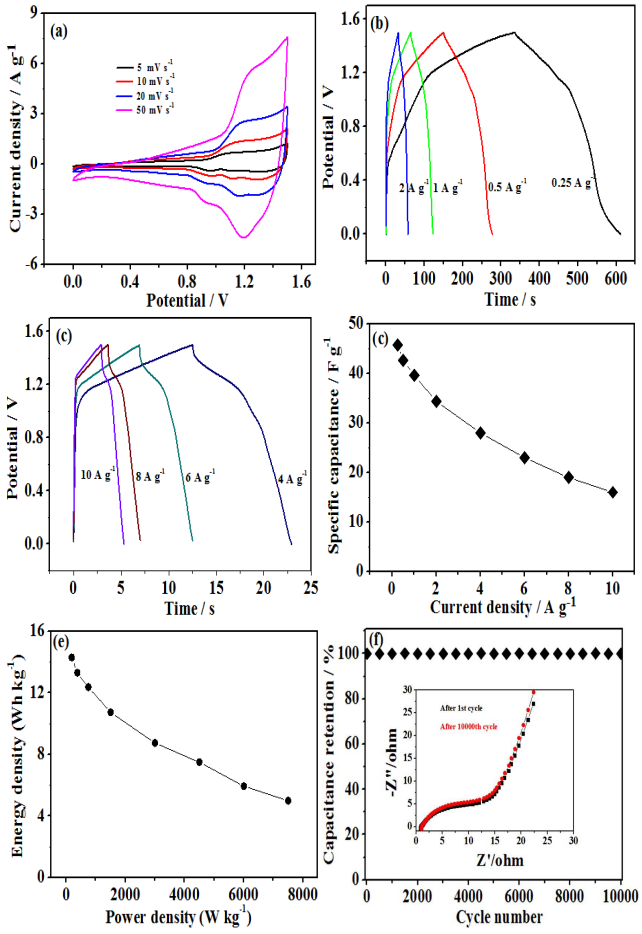

Fig. 6. (a) CV curves, (b, c) charge–discharge curves, (d) capacitances versus current densities, (e) energy and power density and (f) variation of capacitance with cycle number at 4 A g^{-1} of the Co_3O_4 rugby balls//graphene hydrogels asymmetric supercapacitor. The inset is EIS spectra after 1st and 10000th cycle.

In summary, we firstly synthesized mesoporous Co_3O_4 rugby balls using a simple solvothermal/calcination process. Such rugby balls possess excellent electrochemical performance and is suitable as advanced electrode material for pseudosupercapacitors. When the mesoporous Co_3O_4 rugby balls and 3D graphene hydrogels are formed to be an asymmetric supercapacitor, high energy density and power density, as well as a super-long cycle life have been achieved. These findings promote new opportunities for mesoporous Co_3O_4 rugby balls as high-performance supercapacitors and other energy-storage devices.

Acknowledgements

The authors would like to thank the Chemistry Experimental Centre at the Tongji University for providing characterization equipment and assistance..

Notes and references

Department of Chemistry, Tongji University, Shanghai 200092, China. Tel.: +86 02165982654x8430; fax.: +86 02165982287; E-mail: xzj@tongji.edu.cn.

† Electronic Supplementary Information (ESI) available: [Experimental details]. See DOI: 10.1039/b000000x/

1 J. R. Miller, R. A.Outlaw and Holloway, B. C. *Science* 2010, **329**, 1637.
2 M. D. Stoller and R. S. Ruoff, *Energy Environ. Sci*. 2010, **3**, 1294.
3 H. Wang, H. S. Casalongue, Y. Liang and H. Dai. *J. Am. Chem. Soc*. 2010, **132**, 7472.
4 W. Chen, R. B. Rakhi, L. Hu, X. Xie, Y. Cui and H. N. Alshareef, *Nano Lett*., 2011, **11**, 5165.
5 Y. Lu, X. Wang, Y. Mai, J. Xiang, H. Zhang, L. Li, C. Gu, J. Tu and S. X. Mao, J. Phys. Chem. C 2012, 116, 22217.
6 C. C. Hu, K. H. Chang, M. C. Lin and Y. T. Wu, *Nano Lett*., 2006, **6**, 2690.
7 H. Wang, Y. Wang and X. Wang, *Electrochem. Commun*. 2012, **18**, 92.
8 R. Tummala, R. K. Guduru and P. S. Mohanty, *J. Power Sources*, 2012, **209**, 44.
9 H. W. Wang, Z. A. Hu, Y. Q. Chang, Y. L. Chen, Z. Q. Lei, Z. Y. Zhang and Y. Y. Yang, *Electrochim. Acta* 2010, **55**, 8974.
10 H. Xia, M. O. Lai and L. Lu, *J. Power Sources* 2011, **196**, 2398.
11 M. B. Zheng, J. Cao, S. T. Liao and J. S. Liu, H. Q. Chen, Y. Zhao, W. J. Dai, G. B. Ji, J. M. Cao, J. Tao, *J. Phys. Chem. C* 2009, **113**, 3887.
12 L. R. Hou, C. Z. Yuan, L. Yang, L. F. Shen, F. Zhang and X.G. Zhang, *RSC Adv*. 2011, **1**, 1521.
13 Y. Wang, Z. Y. Zhong, Y. Chen, C. T. Ng and J. Y. Lin, *Nano Res.* 2011, 4, 695.
14 D. Zhang and W. Zou, *Current Applied Physics* 2013, **13**, 1796.
15 B.R. Duan and Q. Cao, *Electrochim. Acta* 2012, 64, 154.
16 J. Xu, L. Gao, J. Y. Cao, W. C. Wang and Z. D. Chen, *Electrochim. Acta* 2010, **56**, 732.
17 F. Zhang, C. Yuan, X. Lu, L. Zhang, Q. Chea and X. Zhang, *J. Power Sources*, 2012, **203**, 250.
18 S. K. Meher and G. R. Rao, *J. Phys. Chem. C* 2011, **115**, 15646.
19 W. Du, R. Liu, Y. Jiang, Q. Lu, Y. Fan and F. Gao, *J. Power Sources* 2013, **227**, 101.
20 T. Y. Wei, C. H. Chen, K. H. Chang, S. Y. Lu and C. C. Hu, *Chem. Mater.* 2009, **21**, 3228.
21 F. Cao, G. X. Pan, P. S. Tang and H. F. Chen, *J. Power Sources* 2012, **216**, 395.
22 Y. F. Yuan, X. H. Xi, J. B. Wu, X. H. Huang, Y. B. Pei, J. L. Yang and S. Y. Guo, *Electrochem. Commun.* 2011, **13**, 1123.
23 S. L. Xiong, C. Z Yuan and X. G. Zhang, B. J. Xi, Y. T. Qian, *Chem. Eur. J.* 2009, **15**, 5320.
24 Y. Wang, H. Wang and X. Wang, *Electrochim. Acta* 2013, **92**, 298.
25 X. Xia, J. Tu, Y. Zhang, X. Wang, C. Gu, X. Zhao and H. J. Fan, *ACS Nano*, 2012, **6**, 5531.
26 J. Liu, J. Jiang, C. Cheng, H. Li, J. Zhang , H. Gong and H. J. Fan, *Adv. Mater*. 2011, **23**, 2076
27 H. B. Li, M. H. Yu, F. X. Wang, P. Liu, Y. Liang, J. Xiao, C. X. Wang, Y. X. Tong and G. W. Yang, *Nat. Commun*. 2013, **4**, 1894.
38 X. Xia, D. Chao, Z. Fan, C. Guan, X. Cao, H. Zhang and H. J. Fan, *Nano Lett*., 2014, **14**, 1651.
39 H. Wang, H. Yi, X. Chen and X. Wang, *J. Mater. Chem. A*, 2014, **2**, 3223.
30 L. Zhang and G. Shi, *J. Phys. Chem. C* 2011, **115**, 17206.
31 J. W. Lang, L. B. Kong, M. Liu, Y. C. Luo and L. Kang, *J. Solid State Electron*. 2010, **14**, 1533.
32 Z. S. Wu, W. Ren, D. W. Wang, F. Li, B. Liu and H. M. Cheng, *ACS Nano* 2010, **4**, 5835.
33 X. Wang, W. S. Liu, X. H. Lu and P. S. Lee, *J. Mater. Chem.* 2012, **22**, 23114.

TOC

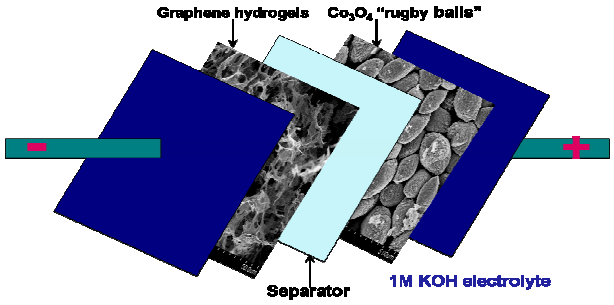

Mesoporous Co_3O_4 rugby balls for the asymmetric supercapacitor manifest high energy/power density and no decay after 10,000 cycles.